Proceedings of the IEEE
International Conference on Mechatronics & Automation
Niagara Falls, Canada • July 2005

Actuation Scheduling in Mobile Actuator Networks for Spatial-Temporal Feedback Control of A Diffusion Process With Dynamic Obstacle Avoidance

YangQuan Chen, *Senior Member, IEEE*, Zhongmin Wang and Jinsong Liang, *Student Members, IEEE*

Center for Self-Organizing and Intelligent Systems (CSOIS)
Dept. of Electrical and Computer Engineering
4160 Old Main Hill, Utah State University, Logan, UT 84322-4160, USA

***Abstract*— In this paper, we discuss the problem of path planning for a group of networked mobile robots which can release neutralizing chemicals, known as "mobile actuator networks", to neutralize the toxic 2D diffusion process modelled by a parabolic PDE distributed parameter system. The desired trajectory of the robot is decided by Centroidal Voronoi Tessellations. Potential field method is used for the mobile robots to avoid dynamic obstacles in its working space. Simulation results show the effectiveness of our proposed method.**

***Index Terms*— Diffusion process, pollution neutralization, Centroidal Voronoi Tessellation, distributed parameter system simulation, potential field.**

I. Introduction

Mobile Actuator/Sensor network has gained intensive research interest in the recent years. By introducing the mobile actuaors/sensors into the wireless sensor network, people can reduce the system cost, increase the robustness and efficiency of the system and provide redundancy, self-configuration and flexibility of the system. Mobile Actuator/Sensor Network (MAS-net) project [1] developed at CSOIS, Utah State University, is a project that uses the small-scale mobile robots for the spatially evolving diffusion process monitoring and control [1], [2], [3]. This project combines mobile robotics with the wireless sensor networks. Each robot has limited sensing ability and limited communication ability. They are expected to coordinate with each other to control the diffusing process by temporal-spatial feedback closed-loop control. Some research challenges and opportunities are presented in [4].

In this paper, we consider the pollution neutralization in MAS-net project. The scenario is described as follows: A toxic diffusion source is releasing toxic material in 2D plane. The diffusion process is modelled as a parabolic PDE system. Chemical concentration sensors are deployed to cover the polluted area and collect data about the pollution. Then, a few of mobile robots equipped with controllable dispensers of neutralizing chemicals are sent to the polluted area with the mission to eliminate the pollution by properly releasing the neutralizing chemicals. In our previous work [5], we try to solve the problem how to choose the optimal positions for these robots and the trajectories the robots will follow when the dynamic diffusion is evolving. In this paper, we extend our previous work and deal with the moving obstacle avoidance in the working space for the robots. Potential field method is used for the individual robot path planning with obstacle avoidance together with centroidal Voronoi tessellation for spatial-temporal control.

As in [5], what we most concern here is the minimal impact to the natural environment for both the pollution and neutralization process. The pollution can have severe negative impact on the the natural environment, the neutralizing chemicals may also have negative impact on the natural environment [6], such as in acid-alkaline neutralization. If the neutralizing chemicals are released too much or too fast, we can not preserve the unaffected area as much as possible. So, one of our objective is to deploy the robots and control the releasing process in an optimal way to minimize any negative impact on the environment. On the other hand, the neutralizing chemicals should be released in such a way that the diffusion of the pollution is bounded so that the heavily affected area is kept as small as possible. These all depend on how the robots positions are chosen, how they move and what the control law is to release the neutralizing chemical. At the same time, to ensure the safety of the robots, the obstacle avoidance should be considered. The mechanism for the obstacle avoidance should be designed in such a way that it does not have significant effect on the feedback control of the diffusion process. Therefore, the problem of area coverage, robot motion planning and the dynamic diffusion process are fundamentally interrelated.

Our research is related to other research topics, for example, the area coverage problem by using mobile robots [7], the applications of Voronoi Diagram in sensor network coverage [8], [9], [10], [11] and Centroidal Voronoi Tessellation in sensor deployment [12]. Our research is also related to the feedback control in PDE systems [13], [14], the application of potential field method in sensor coverage [7] and obstacle avoidance [15], [16]. In [10], [11], Voronoi Diagram and its dual form, the Delaunay triangulation are used to solve the maximal breach problem and maximal support problem in wireless sensor networks. It is pointed out in [11] that the maximal breach path must lie on the line segments of the Voronoi diagram corresponding to the sensors while the maximal support path must lie on the lines of the Delaunay triangulation of the senors. A distributed method has been put forward in [10] to proximately construct the Delaunay tribulations in wireless sensor network.

Motivated by the application of Centroidal Voronoi Tessellation (CVT) in optimal placement of resource [17] and in coverage control of mobile sensing networks [12], we proposed a practical algorithm based on CVT to solve the problem of actuator motion planning to neutralize the pollution. An application of CVT in feedback control system can be found in [14]. In [14], the sensor location problem in feedback control of the partial differential equation system is solved by CVT. The functional gains are served as the density functions in CVT. In our experiment, the pollution concentration is given by the sensors that cover the area and form a mesh. In [15], [16], the potential field method is extended to considered the relative velocity between the robot and the moving obstacle. This method is used in this paper for the robot to avoid dynamic obstacles in the working space. A simulation platform called `Diff-MAS2D` [18] has been developed for measurement scheduling and controls in distributed parameter systems with moving sensors and actuators. Our proposed algorithm has been implemented on `Diff-MAS2D`. Based on our previous work on [5], our new contribution in this paper is that

Corresponding author: Prof. YangQuan Chen, Center for Self-Organizing and Intelligent Systems, Dept. of Electrical and Computer Engineering, 4160 Old Main Hill, Utah State University, Logan, UT 84322-4160. **T**: (435)7970148, **F**: (435)7973054, **W**: `www.csois.usu.edu`, **E**: `yqchen@ece.usu.edu`.

[1] `http://mechatronics.ece.usu.edu/mas-net/`

we give a new distributed algorithm based on Gabriel graph [19] to proximately construct the Voronoi diagram with improved efficiency and we successfully apply the extended potential field method for the robots to avoid moving obstacles.

The remaining part of this paper is organized as follows: In Sec. II, the problem formulation is presented and some related properties of CVT are described. Sec. III is devoted to introducing our simulation platform `Diff-2D` for PDE system measurement and control with sensors and mobile actuators. Then in section IV, we present the algorithms for robot location and introduce the potential field method from [15] for dynamic obstacle avoidance. To show the effectiveness of our proposed method, simulation results are presented in Sec. V. Finally, conclusions and future research directions are presented in Sec. VI.

II. Problem formulation of diffusion neutralization

In this section, the problem of robot optimal position and trajectory generation in feedback control for pollution neutralization is formulated.

Let Ω be a convex polytope in $\mathcal{R}^2$, including its interior. A concentration function is a map $\rho(x, y) : \Omega \to \mathcal{R}_+$ that represents the pollutant concentration over Ω. To simplify the presentation of our main idea, in our simulation experiment, we assume $\rho(x, y)$ is governed by the following PDE system:

$$\frac{\partial \rho}{\partial t} = k \left(\frac{\partial^2 \rho}{\partial x^2} + \frac{\partial^2 \rho}{\partial y^2} \right) + f_d(\rho, x, y, t), \tag{1}$$

where k is a constant positive real system parameter; $f_d(\rho, x, y, t)$ represents the source of the pollution. Currently, there is no control input applied to the system. We assume that the diffusion process is evolving slowly.

Let $P = (p_1, \cdots, p_n)$ be the location of n actuators and let $|\cdot|$ denote the Euclidean distance function. Every robot at p_i will receive information of sensors and release the neutralization chemical by some control law. The objectives are:

- Control the diffusion of the pollution to a confined area.
- Neutralize the pollution in a time optimal way while not making the area overdosed.
- Minimize the polluted area that is heavily affected.

n robots will partition Ω into a collection of n polytopes $\mathcal{V} = \{V_1, \cdots, V_n\}$, $p_i \in V_i$, $V_i \cap V_j = \emptyset$ for $i \neq j$ and $\cup_{i=1}^{n} \bar{V}_i = \bar{\Omega}$ ($\bar{V}_i = V_i \cup \partial V_i$ and $\bar{\Omega} = \Omega \cup \partial\Omega$). It can be seen that to control the diffusion process and minimize the heavily affected area, the robots should be close to those areas with high pollution concentrations so that the pollution can be neutralized timely and does not diffuse further. They can be far from the lightly polluted areas. But putting all robots very close to the pollution source is not a good strategy, because the diffused pollutants that are far away from the source can not be neutralized timely. To decide the positions of the robots, we consider the minimizing of the following cost function

$$\mathcal{K}(P, \mathcal{V}) = \sum_{i=1}^{n} \int_{V_i} \rho(q)|q - p_i|^2 dq \text{ for } q \in \Omega. \tag{2}$$

It is clear that to minimize $\mathcal{K}$, the distance $|q - p_i|$ should be small when the pollution concentration $\rho(q)$ is big. It is the concentration function $\rho(q)$ that determines the optimal positions of the robots. A necessary condition for $\mathcal{K}$ to be minimized is that $\{p_i, V_i\}_{i=1}^{k}$ is a Centroidal Voronoi Tessellation of Ω [20]. For details about Vironoi diagram and Centroidal Voronoi Tessellation, please refer to [20]. What we need to point out is that our algorithm is based on a discrete version of (2). We assume the robots know the positions of sensors within its communication range and can access them. The concentration information of the pollution comes from the measurements of the static, low-cost sensors.

Centroidal Voronoi Tessellation has broad applications in many fields. It is the solution to optimal placement of resources [20], but in general, CVT can only be approximately constructed. For algorithms to implement CVT, refer to [20]. In [17], an example is given to show how CVT can be used to predict the cell divisions. It is shown that, after the cell division process, the new cells' shapes are very closely approximated by Centroidal Voronoi Tessellations corresponding to the increased number of generators. This is an example to show how CVT can be applied in a dynamically evolving environment.

III. Simulation Platform `Diff-MAS2D` [18]

In this section, we give a brief introduction of our simulation platform, `Diff-MAS2D` [18] for simulation of measurement scheduling and controls in distributed parameter systems with moving sensors and moving actuators that other mathematical tools, for example, MATLAB PDE Toolbox [21], FEMLAB [22], Nastran [23], ANSYS [24] can not solve easily.

Specifically, `Diff-MAS2D` is used to solve the following parabolic PDE:

$$\frac{\partial \rho}{\partial t} = k \left(\frac{\partial^2 \rho}{\partial x^2} + \frac{\partial^2 \rho}{\partial y^2} \right) + f(\tilde{\rho}, x, y, t), \tag{3}$$

where $\rho = \rho(x, y, t)$ is the variable to be controlled; $0 \le x \le 1$ and $0 \le y \le 1$ is the spatial domain; $t \ge 0$ is the time domain; k is a positive real constant system parameter; $f(\tilde{\rho}, x, y, t)$ is a combination of control and disturbances (pollution source).

$$f(\tilde{\rho}, x, y, t) = f_c(\tilde{\rho}(x, y, t), x, y, t) + f_d(x, y, t),$$

where $\tilde{\rho}(x, y, t)$ is the measured data of $\rho(x, y, t)$ from the movable sensors; $f_c(\tilde{\rho}(x, y, t), x, y, t)$ is the control applied by the movable actuators; $f_d(x, y, t)$ is the disturbance to model the pollution source. The exact format of $f_c(\tilde{\rho}(x, y, t), x, y, t)$ depends on the closed-loop control law designed by the user based on certain control performance requirement.

Arbitrary combination of the following two types of boundary conditions can be used as boundary conditions for each boundary ($x = 0$, $x = 1$, $y = 0$, and $y = 1$).

- Dirichlet boundary condition

$$\rho = C \tag{4}$$

  where C is a real constant.
- Neumann boundary condition

$$\frac{\partial \rho}{\partial n} = C_1 + C_2 \rho \tag{5}$$

  where C_1 and C_2 are two real constants; n is the outward direction normal to the boundary.

`Diff-MAS2D` uses finite-difference method to discretize the spatial domain of the diffusion equation and leaves the time domain integration to Matlab/Simulink. This scheme enables both `Diff-MAS2D` designers and end-users to make fully use of the capabilities of Matlab/Simulink. The whole function set of Matlab and Matlab Toolbox is available to the end users in designing sensor/actuator trajectories and designing the control laws of the actuators to control the diffusion process. In `Diff-MAS2D`, any number of mobile sensors/actuators can be deployed.

IV. Algorithms for Robot Path Planning

A. Proposed Optimal Actuator Locations Algorithms

First, we describe the algorithms to compute the locations of robots by Centroidal Voronoi Tessellations. Lloy's method is a deterministic algorithm for determining Centroidal Voronoi Tessellations and is described below [20]:

Given a region Ω, a density function $\rho(x)$ defined for all $x \in \bar{\Omega}$, and a positive integer k

1) Select an initial set of k points $\{z_i\}_{i=1}^{k}$ as the generators.
2) Construct the Voronoi sets $\{V_i\}_{i=1}^{k}$ associated with generators $\{z_i\}_{i=1}^{k}$;
3) Determine the mass centroids of the Voronoi sets $\{V_i\}_{i=1}^{k}$; these centroids form the new set of points $\{z_i\}_{i=1}^{k}$;
4) If the new points meet some convergence criterion, terminate; other wise, return to step 2.

Although the CVT is used to solve the static resource location problem, if the diffusion process evolves slowly compared with the convergence rate of the Lloy's method and the control efforts, CVT is still a valid solution to our problem, as verified in our simulation results presented in Sec. VI. The Lloy's method will be executed periodically so that the motion of the robots can be adaptive to the evolution of the diffusion process.

Lloyd's method converges fast but it has higher computation requirements for each iteration. In many applications, the robot has only limited communication abilities. To avoid communication collision and reduce computation requirement, a distributed asynchronous algorithm to construct the Voronoi diagram based on local information is clearly more desirable. Here we give a new a new algorithm to proximally construct the Voronoi diagram based on Gabriel graph. Refer to [19] for details on Gabriel graph. Assume each robot can communicate with other robots within the radius R_i. R_i can be an adjustable communication parameter. *disk*(*i, j*) is a disk area whose center is the center of the line between robot *i* and robot *j*. Its radius is $\frac{1}{2}|p_i - p_j|$. In the step 2 of the above Lloy's algorithm, each robot will perform:

1) Find other robots within R_i, these robots are its neighbors and form a set $\mathcal{N}(i)$.
2) For each robot $j \in \mathcal{N}(i)$, if the *disk*(*i,j*) does not include any other robots, robot *i* recognizes robot *j* as its neighbor in Voronoi diagram. They share a common Voronoi edge.
3) Use the property that a shard Voronoi edge of robot *i* and *j* is the perpendicular bisector line of the segment between robot *i* an robot *j*, the Voronoi cell for robot i can be constructed explicitly.
4) For each Voronoi vertex of the cell v_i, find $r_i = \max|p_i - v_i|$.
5) Find all sensors within radius r_i and within the voronoi cell.

Base on the properties of Gabriel graph, this algorithm can construct a diagram that can closely approximate the Voronoi diagram. This algorithm is more efficient that the method used in [5], because robot *i* does not need to inquiry every sensor within radius R_i and the corresponding computation requirement is also removed. We have to point out that R_i should be big enough to have a good approximation.

B. Repulsive Potential Field for Obstacle Avoidance

In this section, we consider the safety issue of the mobile robots. It is highly likely that the robot will encounter moving obstacles that travel through the polluted area, for example, the moving cargo vessels. In order to avoid collision between the robot and the moving obstacle effectively, the relative position and velocity between robot and obstacle should be considered. Here we introduce a potential field method from [15] that is used in this paper for dynamic obstacle avoidance.

Let $\mathbf{p}$ and $\mathbf{v} = \dot{\mathbf{p}}$ denote the position and the velocity of the robot, respectively. Assume the robots can obtain the position $\mathbf{p}_{obs}$ and the velocity $\mathbf{v}_{obs}$ of the obstacle. Then the relative velocity v_{RO} between the robot and the obstacle in the direction from the robot to the obstacle is given by:

$$v_{RO} = [\mathbf{v}(t) - \mathbf{v}_{obs}(t)]^T \mathbf{n}_{RO}. \tag{6}$$

where $\mathbf{n}_{RO}$ is a unit vector pointing from the robot to the obstacle. Note that if $v_{RO} \leq 0$, then the robot is moving away from the obstacle and no avoidance is needed.

Consider the actuator saturation, the maximum acceleration/deceleration of the robot is given by a_{max}. Then the distance the robot will trave when it reaches zero velocity at maximum deceleration is:

$$\rho_m = \frac{v_{RO}^2}{a_{max}}. \tag{7}$$

In [15], the repulsive potential generated by the obstacle is given by:

$$U_{rep}(\mathbf{p}, \mathbf{v}) = \begin{cases} 0: \\ \text{if } \rho_s(\mathbf{p}, \mathbf{p}_{obs}) - \rho_m \geq \rho_0 \text{ or } v_{RO} \leq 0 \\ \eta(\frac{1}{\rho_s(\mathbf{p},\mathbf{p}_{obs}) - \rho_m} - \frac{1}{\rho_0}): \\ \text{if } 0 < \rho_s(\mathbf{p}, \mathbf{p}_{obs}) - \rho_m < \rho_m \text{ and } v_{RO} > 0 \\ \text{undefined}: \\ \text{if } v_{RO} > 0 \text{ and } \rho_s(\mathbf{p}, \mathbf{p}_{obs}) < \rho_m \end{cases} \tag{8}$$

where $\rho_s(\mathbf{p}, \mathbf{p}_{obs})$ is the distance between the robot and the obstacle; $\rho_0 > 0$ is the influence range of the repulsive force for obstacle avoidance; η is a positive designing parameter.

Let $\mathbf{n}_{RO\perp}$ be the unit vector perpendicular to $\mathbf{n}_{RO}$ and $\mathbf{n}_{RO\perp}^T n_{RO\perp} = 1$. The positive force between the robot and the obstacle is defined as the negative gradient of the repulsive potential with respect to the robot position and velocity:

$$F_{rep}(\mathbf{p}, \mathbf{v}) = \begin{cases} 0: \\ \text{if } \rho_s(\mathbf{p}, \mathbf{p}_{obs}) - \rho_m \geq \rho_0 \text{ or } v_{RO} \leq 0 \\ \mathbf{F}_{rep1} + \mathbf{F}_{rep2}: \\ \text{if } 0 < \rho_s(\mathbf{p}, \mathbf{p}_{obs}) - \rho_m < \rho_m \text{ and } v_{RO} > 0 \\ \text{undefined}: \\ \text{if } v_{RO} > 0 \text{ and } \rho_s(\mathbf{p}, \mathbf{p}_{obs}) < \rho_m \end{cases} \tag{9}$$

where:

$$F_{rep1} = \frac{-\eta}{(\rho_s(\mathbf{p}, \mathbf{p}_{obs} - \rho_m(v_{RO}))^2}(1 + \frac{v_{RO}}{a_{max}})\mathbf{n}_{RO}.$$

and

$$F_{rep2} = \frac{\eta v_{RO} v_{RO\perp}}{\rho_s(\mathbf{p}, \mathbf{p}_{obs}) a_{max}(\rho_s(\mathbf{p}, \mathbf{p}_{obs}) - \rho_m(v_{RO}))^2}\mathbf{n}_{RO\perp}.$$

where $v_{RO\perp}$ is given by

$$v_{RO\perp} = \sqrt{\| \mathbf{v}(t) - \mathbf{v}_{obs} \|^2 - v_{RO}^2(t)}.$$

The mobile robots are treated as virtual particles with unit mass and obey the second-order dynamical equation:

$$\ddot{p}_i = F_i$$

where the control input F_i is given by

$$F_i = f_i - k_v \dot{p}_i + F_{rep} \tag{10}$$

with f_i the force input to control the motion of the robot by CVT. f_i is given by a proportional control law:

$$f_i = -k(p_i - \bar{p_i})$$

where $\bar{p_i}$ is the computed mass centroid of the current Voronoi cell.

The second term of (10) on the right hand side is the viscous friction artificially introduced [25]. k_v is the friction coefficient and $\dot{p}_i$ denotes the velocity of the robot i. This term is used to eliminate the oscillation behavior of robots described in [8] when the robot is close to its destination. The viscous term assures that in the absence of the external force, the robot will come to a standstill eventually. The robot actuator will saturate if $\| F_i \| \geq a_{max}$.

We have to point out that the motion control of robots based on CVT does not need to consider the possible collision between robots. Every time the robots moves, it moves within its cell decided by the

Voronoi diagram and the cells do not overlap, so the possibility that two robots will run into each is 0.

We can also use proportional control for the neutralizing chemical releasing. The amount of chemicals each robot released is proportional to the average pollutant concentration in the Voronoi cell belonging to that robot. Although our simulation is model-based, our control algorithms for each robot are not relying on the exact model information. They are based only on the sensor information each robot can access.

V. Simulation Results

`Diff-MAS2D` is used as the simulation platform for our implementation. The area concerned is given by $\Omega = \{(x,y)|0 \le x \le 1, 0 \le y \le 1\}$.

The system with control input is modelled as

$$\frac{\partial \rho(x,y,t)}{\partial t} = k(\frac{\partial^2 \rho(x,y,t)}{\partial x^2} + \frac{\partial^2 \rho(x,y,t)}{\partial y^2}) + f_c(x,y,t) + f_d(x,y,t), \tag{11}$$

where $k = 0.01$ and the boundary condition is given by

$$\frac{\partial u}{\partial n} = 0.$$

The stationary pollution source is modelled as a point disturbance f_d to the the PDE system (1) with its position at $(0.75, 0.35)$ and

$$f_d(t) = 20e^{-t}|_{(x=0.75, y=0.35)}.$$

In our simulation, we assume that once deployed, the sensors remain static. There are 29×29 sensors evenly distributed in a square area $(0,1)^2$ and they form a mesh over the area. There are 4 robots that can release the neutralizing chemicals. For the robot motion control, the viscous coefficient is given by $k_v = 1$ and the control input is given by

$$F_i = -3(p_i - \bar{p_i}) - \dot{p}_i + F_{rep}.$$

To generate the repulsive force F_{rep} for obstacle avoidance, we choose the influence range ρ_0 to be 0.05 so that when the obstacle is within the range of ρ_0 to the robot, the motion of the robot will be affected. η is given by 0.04. The maximum acceleration/deceleration of robot is given by $a_{max} = 1$. The pollution source begins to diffuse at $t = 0$ to the area Ω, 4 robots are deployed with initial positions at $(0.33, 0.33), (0.33, 0.66), (0.66, 0.33), (0.66, 0.66)$, respectively. The obstacle will start at $(0.8, 0.03)$ and goes parallel to the y axis until it arrives at $(0.8, 1.0)$. Figure 1 shows the initial positions of the robots, the positions of the sensors, the position of the pollution source and the initial positions of the obstacle.

We choose the simulation time to $t = 5$ sec. and the time step is chosen as $\Delta t = 0.002$ sec. The robot recomputes its desired position every 0.1 sec. and generates its desired trajectory. While at the same time, it try to avoid the moving obstacles by using potential field method. To show how the robots can control the diffusion of the pollutants, the robots begin to react at $t = 0.2$ sec. The system evolves under the effects of diffusion of pollutants and diffusion of neutralizing chemicals released by robots.

Figure 2 to 5 show the evolution of the diffusion process and the movements of robots at $t = 1.0s, 1.3s, 1.8s, 3.9s$, respectively. The left part of the figure is a 3D plot of $\rho(x,y,t)$ and the right part of the figure shows the current position of the robots. In Fig. 2, robots move towards the source of the pollution, while the obstacle is approaching robot 3 and robot 4. Also can be seen there is a peak at the pollution source. In Fig. 3, robot 4 tries to avoid collision with the obstacle by moving along the same direction as the obstacle's. Robot 3 moves to the northeast to tries to avoid the obstacle. Fig. 4 shows that robot 3 and robot 4 successfully avoid the collision with the obstacle. They

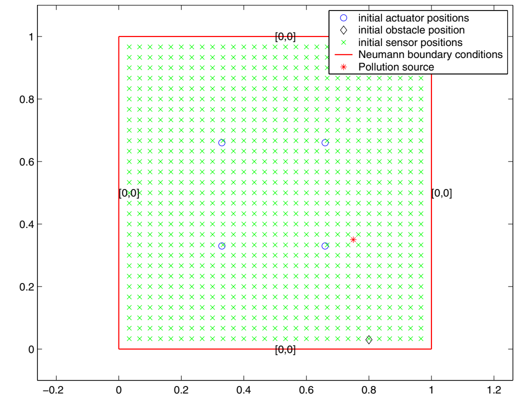

Fig. 1. Initial layout of actuators, sensors and obstacle.

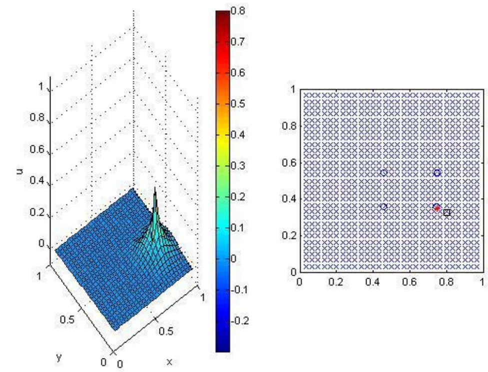

Fig. 2. Evolution of the diffusion process at $t = 1.0$ sec.

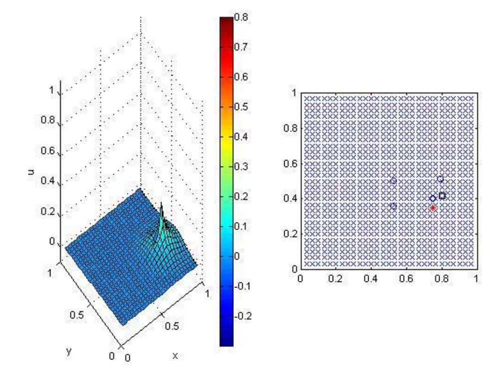

Fig. 3. Evolution of the diffusion process at $t = 1.3$ sec.

move to their destination decided by CVT and try to suppress the diffusion of pollution around its source.

Figure 6 shows the distances between the obstacle and robot 3 and 4. It can be seen that a minimal distance of 0.05 between the robot and the obstacle is guaranteed. And because of the short effective range of the repulsive force, it only has limited effect on the robot motion. Obstacle avoidance does not introduce any significant effect on the feedback control of the diffusion process. Figure 7 shows the trajectories of the robots for $t \le 5$ sec. It can be seen that at first, the robots move towards the pollution source to suppress the diffusion of

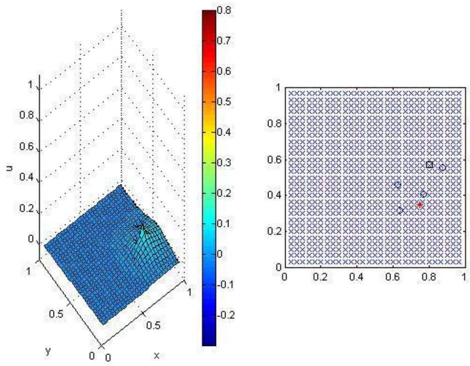

Fig. 4. Evolution of the diffusion process at $t = 1.8$ sec.

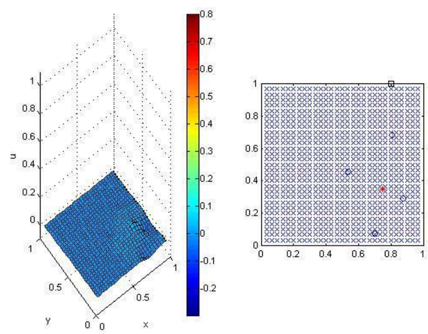

Fig. 5. Evolution of the diffusion process at $t = 3.9$ sec.

the source. And then they move around to track the pollution that has already diffused and try to neutralize it. As also can be seen in Fig. 5, the peak is suppressed and the robots move towards the boundary of Ω.

The evolution of the amount of pollutants are shown in Figure. 8. In Fig. 8, the y axis is the sum of the sensor measurements. It shows that the amount of pollutants decreases to 34% of its peak value at the end of the simulation. And the the decreasing process is monotonic. The evolution of the amount of pollutants without control is also shown in Fig. 8.

Figure 9 shows the evolution of Voronoi diagrams at $t = 0.6s, 1.8s, 3.0s, 4.2s$, respectively.

To show the effectiveness of our proposed algorithm for pollution neutralization, we compare our method based on CVT with the case when 4 robots are uniformly distributed at at $(0.33, 0.33), (0.33, 0.66), (0.66, 0.33), (0.66, 0.66)$ respectively and keep still. The control laws for chemical releasing are the same. We assume that if the concentration of the pollution ranges in $0.02 \geq \rho(x, y, t) \geq -0.001$, it is safe. In Fig. 10, the y axis represents the percentage of sensors whose measurements are at safe level. It can be seen that the safe area increases fast after the control has been implemented by method based on CVT. It means the polluted area can be recovered quickly. While by using evenly distributed deployment, the robots can not recover the polluted area efficiently.

The overall spatial-temporal pollution control results are animated via animated gif file available at
`http://mechatronics.ece.usu.edu/mas-net /movies/zm/icma05a.gif`

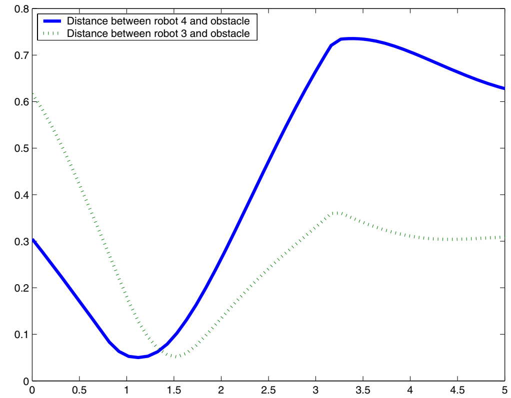

Fig. 6. Distance between the obstacle and the robots

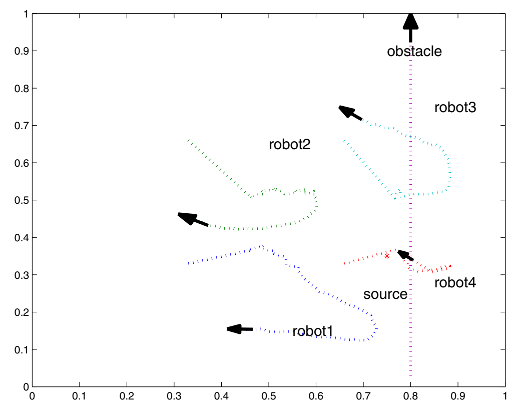

Fig. 7. Robots trajectories

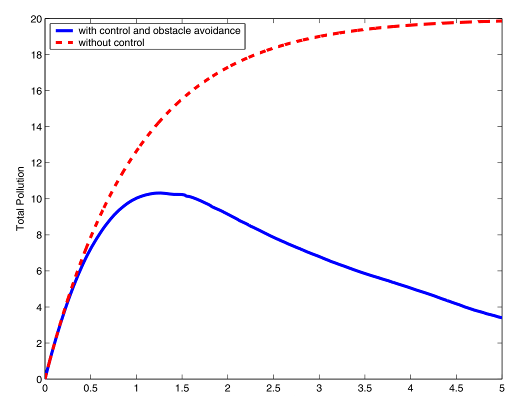

Fig. 8. Evolution of the amount of pollutants.

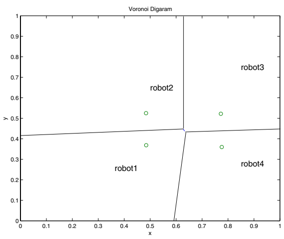

(a) Voronoi diagram at $t = 0.6$ sec.

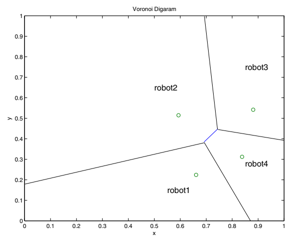

(b) Voronoi diagram at $t = 1.8$ sec.

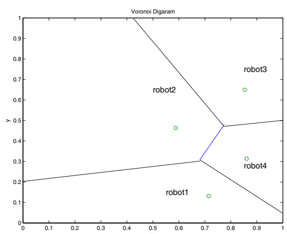

(c) Voronoi diagram at $t = 3.0$ sec.

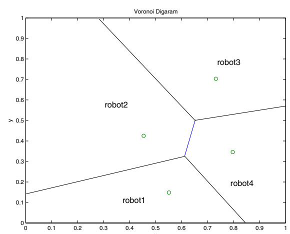

(d) Voronoi diagram at $t = 4.2$ sec.

Fig. 9. Evolution of Voronoi diagrams

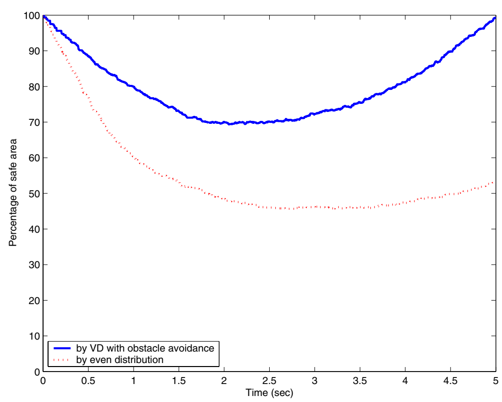

Fig. 10. Comparison of two different robot deployment methods.

VI. Conclusion

In this paper, we extend the application of Centroidal Voronoi Tessellation to pollution elimination by feedback control with moving actuators. Potential field method that considers the object velocity is applied for the robot to avoid moving obstacles in the working space. A simulation platform `Diff-MAS2D` is used to prove the effectiveness of our algorithm. In the future, we will extend our research for pollution feedback control by using mobile sensors and mobile actuators. We will take into account the sensor noise and unreliable communication and attempt to exploit a hybrid model-based and model-free approach.

References

[1] Kevin L. Moore, Yang Quan Chen, and Zhen Song, "Diffusion based path planning in mobile actuator-sensor networks (MAS-net) - some preliminary results," in *Proc. of SPIE Conf. on Intelligent Computing: Theory and Applications II, part of SPIE's Defense and Security*, Orlando, FL., USA, April 2004, SPIE.

[2] YangQuan Chen, Kevin L. Moore, and Zhen Song, "Diffusion boundary determination and zone control via mobile actuator-sensor networks (MAS-net): Challenges and opportunities," in *Proc. of SPIE Conf. on Intelligent Computing: Theory and Applications II, part of SPIE's Defense and Security*, Orlando, FL, Apr. 2004.

[3] Zhongmin Wang, Zhen Song, Peng-Yu Chen, Anisha Arora, Dan Stormout, and YangQuan Chen, "MASmote - a mobility node for MAS-net (mobile actuator sensor networks)," in *Proceedings of 2004 IEEE International Conference on Robotics and Biomimetics*, Shengyang, China, August 22-25 2004, Robio04.

[4] K. L. Moore and Y. Q. Chen, "Model-based approach to characterization of diffusion processes via distributed control of actuated sensor networks," in *Proc. of IFAC Symposium of Telematics Applications in Automation and Robotics, Helsinki University of Technology Espoo, Finland*, 2004.

[5] Yangquan Chen, Zhongmin Wang, and Jinsong Liang, "Optimal dynamic actuator location in distrbuted feedback control of a diffusion process," in *Submitted to IEEE Int. Conf. on Decision and Control (CDC/ECC'05)*, 2005.

[6] H. K. Karapanagioti and As. Atalay, "Laboratory evaluation of ash meterials as acid-distributed land amendments," *Global Nest: the International Journal*, vol. 3, no. 1, pp. 11–21, 2001.

[7] Ioannis Rekleitis, Vincent Lee-Shue, Ai Peng New, and Howie Choset, "Limited communication, multi-robot team based coverage," in *Proceedings of the 2004 IEEE International Conference on Robotics and Automation*, New Orleans, LA, April 2004, pp. 3462–3468.

[8] Nojeong Heo and P. K. Varshney, "Energy-efficient deployment of intelligent mobile sensor networks," *IEEE Transactions on Man and CyberneticsSystems*, vol. Part A, pp. 78 – 92, January 2005.

[9] Mihaela Cardei and Jie Wu, "Coverage in wireless sensor networks," `http://www.cse.fau.edu/~jie/`.

[10] Xiangyang Li, Pengjun Wan, and Ophir Frieder, "Coverage in wireless ad hoc sensor networks," *IEEE Transactions on Computers*, vol. 52, no. 6, June 2003.

[11] S. Meguerdichian, F. Koushanfar, M. Potkonjak, and M.B. Srivastava, "Coverage problems in wireless ad-hoc sensor networks," in *Proceedings of IEEE INFOCOM*, April 2001, pp. 1380–1387.

[12] Timur Karatas Jorge Cortés, Sonia Matínez and Francesco Bullo, "Coverage Control for Mobile Sensing Networks," *IEEE Transactions on Robotics and Automation*, vol. 20, no. 20, pp. 243–255, April 2004.

[13] Jeanne A. Atwell and Belinda B. King, "Reduced order controllers for spatially distributed systems via proper orthogonal decomposition," *SIAM Journal on Scientific Computing*, vol. 26, no. 1, pp. 128–151, 2004.

[14] A. L. Faulds and B. B. King, "Sensor location for feedback control of partial differential equation systems," in *Proceedings of the 2000 IEEE CCA/CACSD*, Anchorage, AK, September 2000, pp. 536 – 541.

[15] S. S. Ge and Y. J. Cui, "Dyanmic motiong planning for mobile robots using potentail field method," *Autonomous Robots*, vol. 13, pp. 207–222, 2002.

[16] A. Poty, P. Melchior, and A. Oustaloup, "Dynamic path planning for mobile robots using fractional potential field," in *Proceedings of the First International Symposium on Control, Communications and Signal Processing*, 2004, pp. 557–561.

[17] Qiang Du, Vance Faber, and Max Gunzburger, "Centroidal Voronoi Tessellations: Applications and Algorithms," *SIAM Review*, vol. 41, no. 4, pp. 637–676, 1999.

[18] Jingsong Liang and YangQuan Chen, "Diff-MAS2D (version 0.9) user's manual: A simulation platform for controlling distributed parameter systems (diffusion) with networked movable actuators and sensors (MAS) in 2D domain," Tech. Rep. USU-CSOIS-TR-04-03, CSOIS, Utah State University, 2004.

[19] K. R. Gabriel and R. R. Sokal, "A new statistical approach to geographic variation analysis," *Systematic Zoology*, vol. 18, pp. 259–278, 1969.

[20] Lili Ju, Qiang Du, and Max Gunzburger, "Probabilistic methods for centroidal Voronoi tessellations and their parallel implementations," *Parallel Comput.*, vol. 28, no. 10, pp. 1477–1500, 2002.

[21] "MATLAB," `http://www.mathworks.com/`.

[22] "Femlab," `http://www.comsol.com/`.

[23] "Nastran," `http://www.nenastran.com`.

[24] "ANSYS," `http://www.ansys.com`.

[25] Andrew Howard, Maja J Mataric, and Gaurav S Sukhatme, "Mobile sensor network deployment using potential fields: A distributed, scalable solution to the area coverage problem," in *Proceedings of the 6th International Symposium on Distributed Autonomous Robotics Systems*, Fukuoka, Japan, June 2002.